JOURNAL OF CATALYSIS **132,** 302–310 (1991)

Monte Carlo Modeling of a Simple Catalytic Reaction Mechanism: Comparison with Langmuir Kinetics

L. V. LUTSEVICH,* V. I. ELOKHIN,† A. V. MYSHLYAVTSEV,‡ A. G. USOV,*
AND G. S. YABLONSKII‡

Computer Center Sib. Br. Acad. Sci. USSR, Novosibirsk; †Institute of Catalysis Sib. Br. Acad. Sci. USSR, pr. acad. Lavrentjeva 5, Novosibirsk, 630090, USSR; and ‡Touvinian Complex Department, Kyzyl, USSR

Received July 5, 1990; revised April 29, 1991

Using a Monte Carlo simulation technique, we have investigated the model of a simple catalytic reaction (the Langmuir–Hinshelwood mechanism)

$$A + Z \xrightarrow{k_1} AZ,\ B_2 + 2Z \xrightarrow{k_2} BZ,$$

$$AZ + BZ \xrightarrow{k_3} AB + 2Z,\ k_3 \rightarrow \infty,$$

under varying intensities of surface diffusion. Having compared the results of the MC simulation with those obtained previously in the model based on the kinetic equations (formulated under the assumption of ideal adsorbed layer, the IAL model), we found the conditions under which both models give identical results. The difference between the results obtained with the IAL and those obtained with the MC model is associated with clustering of the adsorbed substances on the surface. © 1991 Academic Press, Inc.

INTRODUCTION

The mechanisms of catalytic reactions and their elementary stages are investigated by using two types of models: (i) those based on ordinary kinetic equations (system of ODEs, usually based on the Langmuir hypothesis about the ideal adsorbed layer), and (ii) those in which any molecular act is simulated directly by the Monte Carlo (MC) method. As a rule, the results obtained with these two models differ considerably. The questions then arise: what is the reason for these differences and when do both models give identical results? Thus, it is a problem of mutual mapping of the models. Answers to these questions are of great importance for developing MC models, because they permit us to select adequate algorithms for the MC simulation in some cases. On the other hand, MC simulation may be used to prove the validity of the assumptions of the analytical theory.

In this paper we compare in detail the behavior of the ideal adsorbed layer (IAL) model with that of the MC model of catalytic reaction, which occurs in accordance with the Langmuir–Hinshelwood mechanism

$$\begin{aligned} &(1)\quad A + Z \xrightarrow{k_1} AZ \\ &(2)\quad B_2 + 2Z \xrightarrow{k_2} 2BZ \\ &(3)\quad AZ + BZ \xrightarrow{k_3} AB + 2Z \end{aligned} \qquad (1)$$

for the special case $k_3 \rightarrow \infty$. Mechanism (1) corresponds to the CO oxidation reaction on platinum metals (*1–3*). The symbol A denotes a CO molecule, B_2 an O_2 molecule, and Z an active site on the surface.

The IAL model of mechanism (1) (in terms of the law of surface action) was comprehensively investigated in the early 1970s in a series of papers summarized in (*4*). The study of MC models began in 1986 with paper (*5*), and papers (*6–12*) were published in following years. As far as we know, a consistent comparison of the results obtained with the MC model with

0021-9517/91 $3.00
Copyright © 1991 by Academic Press, Inc.
All rights of reproduction in any form reserved.

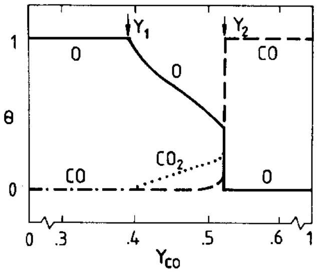

FIG. 1. The average coverage of fractions of O_{ads} (solid lines) and CO_{ads} (dashed lines) and the CO_2 production rates (dotted lines) for steady-state operation, as a function of Y_{CO} (Y_A). Transitions occur at Y_1 and Y_2 (according to (5)).

predictions of the analytical model was carried out only in Refs. (*9, 10*). In paper (*9*) the MC model of mechanism (1) was studied for a finite reaction rate ($k_3 \neq \infty$) in the absence of surface diffusion of the adsorbed particles. The competitive adsorption of reagents and their reaction on the surface appeared to result in an insignificantly inhomogeneous island structure of the adsorbed layer. To describe the results of their MC experiments in terms of the IAL model, some authors (*9*) have considered the fact that particles interact by open boundaries under the clustering, and respectively changed the system of kinetic equations. In (*10*) the MC model of mechanism (1) for the case $k_3 \neq \infty$ was also investigated. It was established that if a reaction rate coefficient dependent on nearest neighbors is used, if this coefficient is included correctly in a scheme of probability calculations, and if there exists a sufficiently high rate of surface diffusion, providing homogeneity of the adsorbed layer, then the results of MC simulation are in very good agreement with the predictions of the IAL model for a wide range of parameters.

The MC model of mechanism (1) for the case $k_3 \to \infty$ without surface diffusion has been comprehensively studied (*5–8*) without comparison with the IAL model. In our paper we have made an attempt to fill this gap. First, we describe the results of the MC model investigation, obtained in (*5–8*), and then we compare them with our results obtained with the same model under limited surface diffusion. We compare both results with the predictions of the IAL model. We show that for the case $k_3 \to \infty$, the MC model's results approach "in the limit" those of the IAL model in two cases: (i) under an increasing surface diffusion intensity *d*; and (ii) under a decreasing level of discreteness (increasing the number of allowable reaction partners *n*). Furthermore, we define for various intensities of surface diffusion a range of parameter $Y_P = P_A/P_{B_2}$ (the ratio of the gas-phase concentration of reactants), where steady-state surface coverages coincide for both the MC and the IAL models.

Let us consider briefly the main results presented in papers (*5–8*), where the MC model of mechanism (1) was studied for the case $k_{-1} = k_{-2} = 0$, $k_3 \to \infty$ in the absence of surface diffusion. In the first paper (*5*), it was established that there exists a range of steady states with a nonzero reaction rate within the interval $Y_1 < Y_A < Y_2$, where $Y_A = P_A/(P_A + P_{B_2})$ is the mole fraction of the *A* reagent in a gas phase, and $Y_1 = 0.389$, $Y_2 = 0.525$ (Fig. 1). Out of this interval the surface is completely covered with either *A* (at $Y_A \geq Y_2$) or *B* (at $Y_A \leq Y_1$) and the reaction rate is equal to zero. The authors of (*5*) called the critical point Y_1, in which *B* surface coverage is continuous, apparently by analogy with accepted classification, the "second-order kinetic phase transition" and the critical point Y_2, in which the coverage undergoes a jump, the "first-order kinetic phase transition." Here we use the same terminology. A percolation threshold of *B* atom coverage close to the Y_2 point in this model was found (*6*). It proved to be achieved at $\Theta_B = 0.525$. This value is significantly less than 0.5927—the percolation threshold for random coverage on a square lattice. Furthermore, in the same paper it was shown that the critical parameters Y_1 and Y_2 do not depend on lattice sizes, at least from the size 40 × 40 (the author employed lattice sizes from 40 × 40 to 240 × 240).

The problem of sizes and types of lattices was investigated in (*7*). The values $Y_1 = 0.3875 \pm 0.0001$ and $Y_2 = 0.5277 \pm 0.0002$ obtained for a square lattice were in very good agreement with the results in (*5*). The authors of (*7*) also established that for a hexagonal lattice there are other critical values: $Y_1 \simeq 0.344$, $Y_2 \simeq 0.561$. For a one-dimensional lattice and for strips one or two sites wide, steady states with nonzero reaction rates were not observed at all (*7*). These steady states begin to appear in strips three sites wide, and the Y_A range of such steady states increases as the strip width increases. Thus, the results presented in (*7*) prove that for narrow and long strips the width (critical geometric size) significantly influences the existence and the size range of steady states with nonzero reaction rates. However, beginning with a certain size (at least 40 × 40 for a square lattice) lattice size does not affect the results, and the differences that arise are associated only with the cell geometry.

Finally, more extensive MC models of mechanism (1), in which diffusion of adsorbed A atoms was taken into account, were investigated (*11, 12*). The increase in A diffusion intensity leads to a shift in the critical point Y_2 up to the maximum value of $Y_A = \frac{2}{3}$ (*12*) and to a further decrease in B coverage at this point.

Let us proceed to the results of the investigation of the IAL model of mechanism (1). We consider the irreversible adsorption case, for which steady-state surface coverages are defined (according to the law of surface action) by

$$\begin{aligned} \dot{\Theta}_A &= k_1P_A\Theta_Z - k_3\Theta_A\Theta_B = 0 \\ \dot{\Theta}_B &= 2k_2P_{B_2}\Theta_Z^2 - k_3\Theta_A\Theta_B = 0, \end{aligned} \qquad (2)$$

where P_A, P_{B_2} are partial pressures of the gas-phase reagents, and $\Theta_Z = 1 - \Theta_A - \Theta_B$, Θ_A, Θ_B are dimensionless concentrations (coverages) of intermediate substances Z, AZ, BZ, respectively. Qualitative analysis of system (2) (*4, 13*) reveals that there always exist two boundary steady states with zero reaction rates, one of which ($\Theta_A = 1$, $\Theta_B = 0$) is stable and another of which ($\Theta_A = 0$, $\Theta_B = 1$) is unstable. In addition, under the conditions

$$2k_2P_{B_2} \geq k_1P_A \quad \text{and}$$

$$k_3(2k_2P_{B_2} - k_1P_A)^2 \geq 8k_1^2P_A^2k_2P_{B_2}, \qquad (3)$$

there exist two internal steady states with nonzero reaction rates, $W = k_3\Theta_A\Theta_B$, located in the reaction polyhedron symmetrically about the $\Theta_A = \Theta_B$ line (*13*). For our case $k_3 \to \infty$ the coordinates of the internal stable steady state with a nonzero reaction rate are

$$\Theta_A = 0, \quad \Theta_B = 1 - k_1P_A/2k_2P_{B_2}. \qquad (4)$$

Setting $k_1 = k_2 = 1$, we obtain $\Theta_B = 1 - Y_P/2$, $\Theta_A = 0$, where $Y_P = P_A/P_{B_2}$. Note that $Y_P = Y_A/(1 - Y_A)$.

Thus, in the IAL model (2) the internal stable steady state (4) exists in the interval of $0 \leq Y_P \leq 2$ ($0 \leq Y_A \leq \frac{2}{3}$) in contrast with the MC model (*5–7*) ($0.3875 \leq Y_A \leq 0.5277$; compare Fig. 4, curves n_∞ and n_4, or Fig. 3, curves d_∞ and d_0).

Summarizing the data from the literature, we can state that the IAL and MC models of mechanism (1) for the case $k_3 \to \infty$ have been investigated comprehensively. Let us note an obvious dissimilarity of the results. The range of steady states with nonzero reaction rates in an IAL model is significantly wider than that in the MC model; the dependencies $\Theta_B(Y_P)$ are different (Fig. 3). In addition, as is clear from (4), in the IAL model there exists a second-order kinetic phase transition (Fig. 3) at the right boundary point $Y_P = 2$ (a bifurcation point where the internal steady-state solution disappears), whereas in the MC model there exists a first-order phase transition at the right boundary point $Y_P = Y_2$. Hence, the second-order kinetic phase transition in an IAL model (2) is shifted to the inner part of the range and becomes a first-order kinetic phase transition. As shown in Fig. 3, a similar shift occurs at the left boundary point ($Y_P = 0 \rightarrow Y_P = Y_1$) at which the second-order kinetic phase transition still remains. We demonstrate below that the dissimilarity of the results of the IAL and MC models is associated with clustering of the adsorbed substance occurring in the MC model with the absence of surface diffusion.

MODELS AND ALGORITHMS DESCRIPTION

We have investigated the model described in (*5*). In this model, as previously pointed out, one-site adsorption of A molecules and two-site dissociative adsorption of B_2 molecules are irreversible. Reagents can leave the surface only in the form of an AB reaction product. Adsorption rate constants k_1 and k_2 are considered to be unity. The only variable parameter is Y_A—the mole fraction of the A reagent in a gas phase. The simulation algorithm is performed as follows. The catalyst surface is represented by a lattice of 100 × 100 sites with periodic boundary conditions and square cells. If a random number W_r uniformly distributed over [0, 1] did not exceed Y_A, then the A molecule adsorption was attempted; otherwise, the B_2 molecule adsorption was attempted. The lattice sites were randomly chosen, and adsorption was allowed only on the blank sites. Each A molecule occupied one site, and each B_2 molecule occupied two adjacent sites (i.e., two sites having a common edge). To select the second vacant site (in the case of B_2 adsorption) only one attempt was made in the randomly chosen direction. As soon as the particle adsorbed all four (or eight in some special experiments) nearest-neighboring sites, they were checked in random order to find the coreagent particle. Under B_2 adsorption such an inspection took place around each of the two occupied sites. As soon as the coreagent particle was found, the adsorbed particles reacted with unity probability. The formed product AB left the surface, thus vacating two sites.

Diffusion in our experiments was simulated as a process of random walks of A molecules and B atoms among vacant lattice sites, as follows. One of four directions was randomly selected for a randomly chosen particle and if the nearest site, corresponding to this direction, was vacant, the particle was made to jump into it. Immediately after that, the search for the reaction partner took place near the new site in the same way as in the adsorption case. The diffusion cycle was inserted into the main one as an inner cycle. After each adsorption attempt occurring in the main cycle (successful or not), the procedure was switched to the diffusion cycle. Thus, the value of the diffusion cycle N in our experiments defines the intensity of surface diffusion d_N (N is the number of diffusion jump attempts per one adsorption attempt).

RESULTS AND DISCUSSION

Keeping in mind that the difference in results obtained with IAL and MC models is associated with clustering of the adsorbed substances, we have investigated the MC model with surface diffusion under varying diffusivity-to-adsorption ratios. The results of these experiments are shown in Fig. 2 along with the results of (*5*) (represented in accordance with our aims) and those of the IAL model (2). It can be seen from Fig. 2 that as a result of increasing diffusion intensity, the curves of steady-

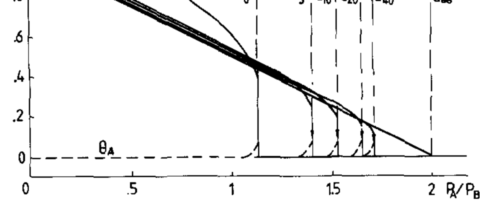

FIG. 2. Dependencies of steady-state coverages on $Y_P = P_A/P_{B_2}$ under varying ratios of adsorption and diffusion intensity (index at d shows value of diffusion cycle); d_0 are the MC results without diffusion (*5*), and d_∞ is the solution of the IAL model (2).

state coverages d_3, d_{10}, d_{20}, d_{40}, obtained by MC simulation, approach the d_∞ straight line, which resulted from the analytical solution (4). At $N \geq 10$, they nearly coincide within a rather large Y_P range. Also in Fig. 2 it is seen that at $N = 3$ already the left critical point $Y_P = Y_1$ shifts to the point $Y_P = 0$ (note that even the low intensity of diffusion eliminates the range with $\Theta_B = 1$) and a further increase in the range of steady states with a nonzero reaction rate occurs only because of the shift of the right critical point Y_2 to the direction of the larger Y_P values. The range $\Delta Y_A = Y_2 - Y_1$ (in terms of Y_A) at varying diffusivity-to-adsorption ratios is

at $N = 0$ $\Delta Y_A \cong 0.14 \pm 0.0002$ (*5, 7*)
$N = 3$ $\Delta Y_A \cong 0.581 \pm 0.001$
$N = 10$ $\Delta Y_A \cong 0.605 \pm 0.001$
$N = 20$ $\Delta Y_A = 0.618 \pm 0.001$
$N = 40$ $\Delta Y_A \cong 0.628 \pm 0.001$.

Let us point out that under these shifts the nature of kinetic phase transitions in the critical points does not alter.

The observed behavior can be accounted for as follows. As is clear from the analytical solution (4), at an infinitely large constant of the reaction rate, the steady-state coverage in the range of $0 \leq Y_P \leq 2$ is formed due to B excess only. In fact, it means that within the mentioned range (at B excess on the surface) all the A molecules adsorbed on the surface instantly react with the neighboring B molecules. The situation presented is a result of the fulfillment of the law of surface action—a principal assumption forming the basis of the model (2). In MC simulation, in the absence of diffusion, the Langmuir hypothesis of an ideal adsorbed layer is not fulfilled and, because the reaction between A–A and B–B pairs is impossible, but occurs with unity probability between A and B pairs, reagent clustering becomes inevitable. Due to the clustering, a reduction in the reaction rate takes place, further storing of the A reagent on the surface occurs, and consequently the first-order kinetic phase transition appears at the Y_2 point (*5*).

Employing diffusion in a MC model leads to an increase in the reaction rate, leads to more complete consumption of the adsorbed A reagent, and favors the formation of coverage as a pure B excess. As long as the given level of diffusion intensity provides the required reaction rate (for the given adsorption rate), the MC curves coincide with the analytical solution (Fig. 2). As soon as the diffusion fails to overcome the increasing rate of A adsorption, the clustering of the A reagent on the surface and a sharp change in coverages occur; i.e., the first-order kinetic phase transition (Y_2 point) appears. It is clear that a further increase in the diffusion intensity to a certain limit, depending on lattice size, will allow one to obtain the full agreement in the IAL and MC models.

Let us consider now peculiarities in the behavior of the MC model at the left critical point Y_1. If diffusion is absent, the mechanism of full B coverage formation is as follows. The single vacant sites ("holes") at the B location eventually become two sites due to A adsorption and further reaction with the neighboring B. The newly formed double sites are then filled preferably with B ($P_{B_2} > P_A$). As long as such a process requires availability of A molecules, the full B coverage evidently can occur only in the range $Y_P \neq 0$. It is for this reason only that the critical point Y_1 is shifted to the right in the absence of diffusion in the MC model. In the presence of diffusion, the picture changes. Each of the double sites obtained from a single site in the manner described above may, due to the diffusion, "break down" into two single sites. Generation of the single sites then takes place. Under the steady-state conditions, it is balanced by the double-site formation occurring when the single sites occasionally meet. In this case a steady-state coverage, at all $Y_P \neq 0$, includes a certain concentration of vacant

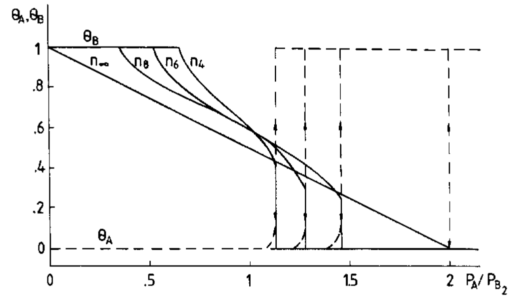

FIG. 3. Dependencies of steady-state coverages on Y_P under varying numbers of allowable reaction partners (index at **n**); **n**$_4$ are the results of (*5*), n_6 those of (*7*), **n**$_8$ those of the present paper, and **n**$_\infty$ is the solution of the IAL model Eq. (2).

sites; i.e., it is not full. The full B coverage at a sufficiently intensive diffusion (at least $N \geq 3$) takes place only at $Y_P = 0$. All this clarifies the peculiarities of the MC model's behavior at the left critical point.

Now we discuss the way in which the discreteness level of the MC model (the number of allowable reaction partners) affects the location of critical points and the width of the steady-state range with the nonzero reaction rate. In (*7*) it was shown that in the absence of diffusion the width of this range and the location of critical points for a lattice with hexagonal ($n = 6$) cells differ from those in a lattice with square ($n = 4$) cells. Representative data from Refs. (*5, 7*) are shown in Fig. 3 (curves n_4, n_6). In Fig. 3 it can be seen that for hexagonal cells widening of the steady-state range with nonzero reaction rate occurs due to the shift of both critical points Y_1 and Y_2 to the corresponding boundary points $Y_P = 0$ and $Y_P = 2$ of the analytical solution (see curves n_4 and n_6). This result may be interpreted as follows. In a lattice with hexagonal cells, each of the particles may have up to six reaction partners (unlike the lattice with square cells, where those cannot exceed four) and hence the reaction rate is higher in this case. The increase in the reaction rate results in the widening of a steady-state range with a nonzero reaction rate, as shown previously in the case of diffusion. Thus, a further increase in the number of allowable reaction partners widens this range even more. To illustrate this we have investigated the MC model (in the absence of diffusion) for the case where the reaction in a lattice with square cells could occur with eight neighbors: the nearest four have a common edge and next-nearest neighbors have a common vertex with the given site. The results are presented in Fig. 3 (curve n_8). Here we can observe a further widening of the steady-state range with a nonzero reaction rate compared to the case with hexagonal cells. Evidently, the increase in the number of allowable reaction partners (the decrease in the discreteness level) causes an MC model to approach an IAL model that has a zero discreteness level (i.e., the maximum number of reaction partners; each particle reacts with any other).

To compare these models in more detail, we have investigated the transient kinetics of steady-state formation for the MC model in the presence of diffusion ($N = 10$). Figure 4 presents the time dependencies of coverages by A and B particles (transitions to the steady state; the initial state was always the pure surface $\Theta_A = \Theta_B = 0$) at various Y_P (more and less than Y_2). Note that two stable steady states (1) $\Theta_A = 0$, $\Theta_B = 1 - Y_P/2$; (2) $\Theta_A = 1$, $\Theta_B = 0$ coexist in the range $0 \leq Y_P \leq 2$; therefore the choice of the initial state determined, in the end, the result of the transient process. From Fig. 4 one can see that near the point $Y_2 \cong 1.53$, where the first-order kinetic phase transition takes place, the time for the steady-state formation drastically increases. If we take the relaxation time (τ_r) as the time when A and B coverages reach steady-state values with 5% accuracy, the τ_r dependence on Y_P will have the peculiarity shown in Fig. 5. This peculiarity corresponds to the critical slowing down near the bifurcation point for the dynamic models (systems of autonomous ordinary differential equations) (*4*). Figure 5 also presents the qualitative dependence of τ_r on Y_P for system

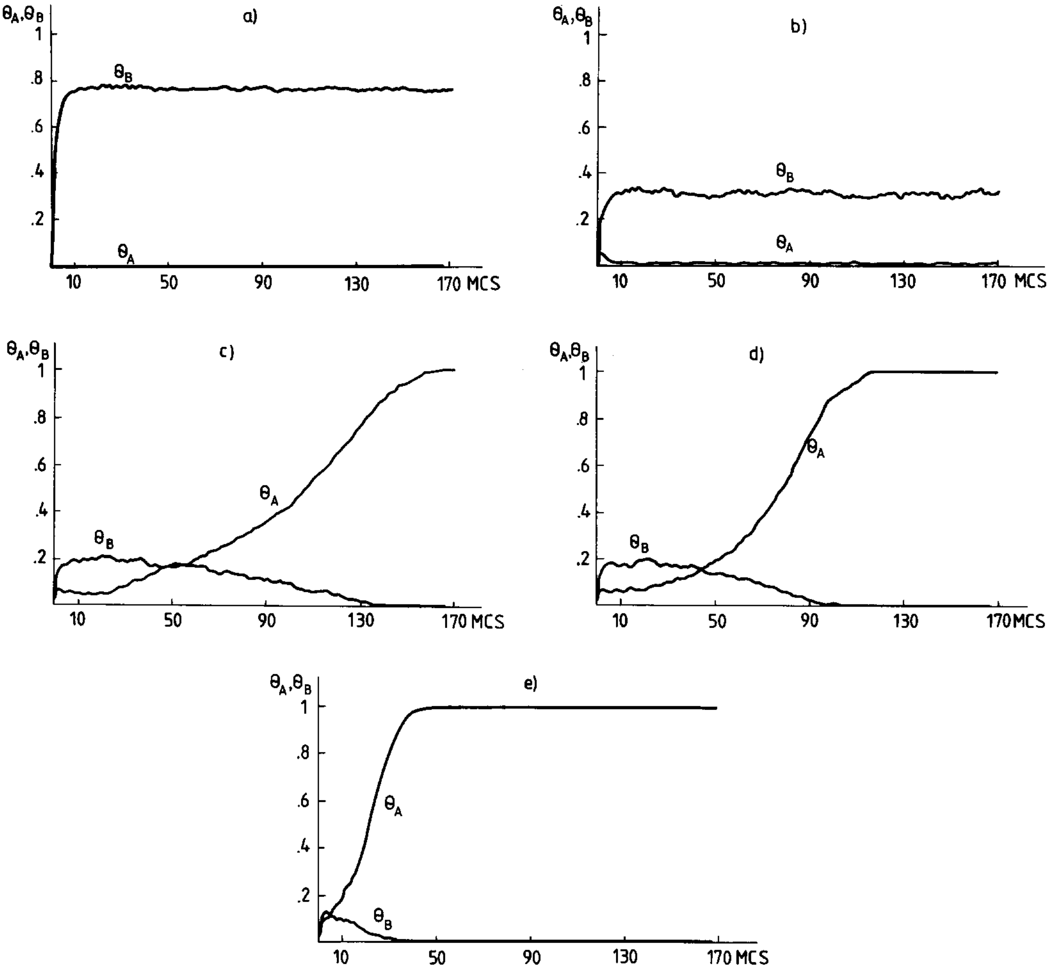

FIG. 4. Transient behavior of Θ_A and Θ_B coverages (via Monte Carlo steps) under varying Y_P: (a) $Y_P = 0.5$; (b) $Y_P = 1.4$; (c) $Y_P = 1.52$; (d) $Y_P = 1.54$; (e) $Y_P = 1.58$. The value of diffusion cycle N = 10.

(2). It is noted that the authors of (*5, 7*) also observed the increase in time of steady-state formation in the absence of diffusion near the Y_2 point. Slow relaxation near the critical points (bifurcations, phase transitions, etc.) seems to be a common feature of dynamic systems, including the MC models.

Now we consider the way in which lattice size influences the location of the Y_2 critical point. Let us introduce the following symbols:

$L_\Theta = \Theta^{-1/2} - 1 \Rightarrow$ the average distance between adsorbed particles for uniform coverage;

$L_L \Rightarrow$ the linear lattice size;

$L_D = N^{1/2} \Rightarrow$ the average distance the particle passes per N random jumps.

Evidently, until the condition $\max(L_D, L_\Theta) \ll L_L$ holds, neither dependence on lattice size will take place. Such a dependence may appear only in the range $\max(L_D, L_\Theta) \sim L_L$. Moreover, for $L_D \gg L_\Theta$ and $L_\Theta \gg L_D$, the dependence on lattice size will be defined by the largest parameter of these

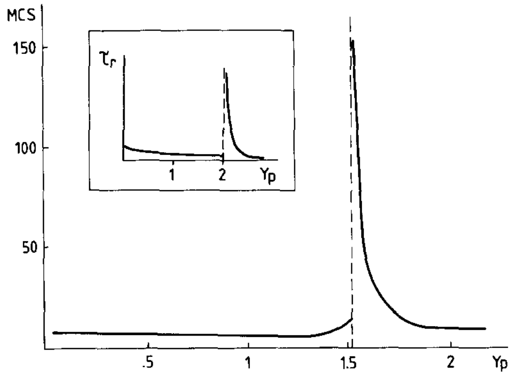

FIG. 5. Dependence of relaxation time (in Monte Carlo steps) on Y_P under transitions from initial state ($\Theta_A = 0$, $\Theta_B = 0$) to the steady state (at N = 10). A qualitative dependence of $\tau(Y_P)$ for the IAL model (2) is shown in the inset.

two, and only in the case $L_D \sim L_\Theta$ will it depend on both.

Let us consider the value $L_\Theta^{\max} = (\Theta_B^{kr})^{-1/2} - 1$, corresponding to the L_Θ value near the critical point Y_2. As can be seen from Fig. 2, in the MC model $L_\Theta^{\max}$ and L_D values are interdependent: an increase in L_D causes a shift in the critical point Y_2 to the right, a decrease in Θ_B steady-state coverage near this point, and an increase in $L_\Theta^{\max}$. Figure 6 presents the dependency of $L_\Theta^{\max}$ on L_D. It is seen that L_D is larger than $L_\Theta^{\max}$ in all cases (except in the range of low diffusion intensity, $L_D \approx 1$) and the curve is well approximated by the linear dependency

$$L_\Theta^{\max} = 0.5 + 0.18 \cdot L_D. \qquad (5)$$

This means that $L_D \gg L_\Theta$ obviously holds for the given model within the range where $L_D > L_\Theta^{\max}$ holds. It follows that the dependency on lattice sizes may appear within the $L_D \sim L_L$ range only. Thus, in our experiments, where a maximal number of diffusion jumps per one adsorption act was considered to be 40 ($L_D \approx 6.32$), this dependence could appear only at $L_L < 10$.

CONCLUSIONS

The difference in results obtained with IAL and MC models is associated with clustering of the adsorbed substances on the surface. This clustering sufficiently influences the kinetics of two-site B_2 adsorption. The adsorption rate of monomolecularly adsorbed reagent A is proportional to the fraction of blank sites Θ_Z, while the adsorption rate of the dissociative adsorbed reagent B_2 is proportional to the fraction of *double* blank sites. However, the fraction of double blank sites can be different for the same Θ_Z, since it is defined by the degree of homogeneity and ordering of the adsorbed layer. It is evident as well that the clustering reduces the reaction in the adsorbed layer since the species within the clusters are not able to react. All of this sharply changes the reaction kinetics and results in the above-mentioned discrepancies in MC and IAL models. The local spatial fluctuations in the adsorbed layer are responsible for clustering in the MC model. To suppress these fluctuations, a sufficiently intensive diffusion is needed (or equivalently, an increase in the allowable number of reaction partners). Note that in the model under study the adsorption mechanism alone does not ensure a homogeneous distribution in the adsorbed layer.

The presented analysis shows that with an increase in diffusion intensity, or with an increase in the allowable number of reaction partners, the MC model of the catalytic mechanism (1) considered in (5–7) ap-

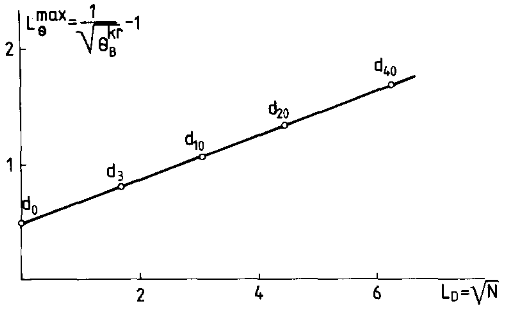

FIG. 6. Dependence of the average distance between adsorbed particles B at Y_2 points on the value of a particle's average displacement for N "diffusion" jumps under varying diffusion intensities d_N.

proaches an IAL model (2) as its limit. Thus the results obtained on the MC model fit the region where the IAL model (2) is valid.

Some complicated phenomena, such as clustering on surfaces, lateral interactions between adsorbed species, modification of surface properties due to the influence of the reaction mixture, precursor adsorption, surface reconstruction, and physicochemical processes on fractal surfaces, can be accounted for easily with MC models. These models can lead to predictions that could not be made through analysis of ordinary kinetic equations.

REFERENCES

1. Engel, T., and Ertl, G., *in* "Advances in Catalysis" (D. D. Eley, H. Pines, and P. B. Weisz, Eds.), Vol. 28, p. 1. Academic Press, San Diego, 1980.
2. Ertl, G., *Surf. Sci.* **152/153,** 328 (1985).
3. Razon, L. E., and Schmitz, R. A., *Catal. Rev.-Sci. Eng.* **28,** 89 (1986).
4. Yablonskii, G. S., Bykov V. I., and Elokhin, V. I., "Kinetics for Model Reactions of Heterogeneous Catalysis." Nauka, Novosibirsk, 1984: Yablonskii, G. S., Bykov, V. I., Gozban, A. I., and Elokhin, V. I., *in* "Kinetic Models of Catalytic Reactions," (R. G. Compton, Ed.), Vol. 32. Elsevier, Amsterdam, 1991. (English)
5. Ziff, R. M., Gulari, E., and Barshad, Y., *Phys. Rev. Lett.* **56,** 2553 (1986).
6. Sadiq, A., *Z. Phys. B, Condensed Matter* **67,** 211 (1987).
7. Meakin, P., and Scalapino, D. J., *J. Chem. Phys.* **87,** 731 (1987).
8. Chopard, B., and Droz, M., *J. Phys. A: Math. Gen.* **21,** 205 (1988).
9. Dumont, M., Poriaux, M., and Dagonnier, R., *Surf. Sci.* **169,** L307 (1986).
10. Araya, P., Porod, W., Sant, R., and Wolf, E. E., *Surf. Sci.* **208,** L80 (1989).
11. Kaukonen, H.-P., and Nieminen, R. M., *J. Chem. Phys.* **91,** 4380 (1989).
12. Ehsasi, M., Matloch, M., Frank, O., Block, J. H., Christmann, K., Rys, F. S., and Hirschwald, W., *J. Chem. Phys.* **91,** 4949 (1989).
13. Bykov, V. I., Yablonskii, G. S., and Elokhin, V. I., *Surf. Sci.* **107,** L334 (1981).